International Journal of Applied Earth Observation and Geoinformation 26 (2014) 36–48

Contents lists available at SciVerse ScienceDirect

International Journal of Applied Earth Observation and Geoinformation

journal homepage: www.elsevier.com/locate/jag

Seasonal comparisons of meteorological and agricultural drought indices in Morocco using open short time-series data

Hicham Ezzine*, Ahmed Bouziane, Driss Ouazar

Equipe d'Analyse des Systèmes Hydrauliques, Département de Génie Civil, Ecole Mohammedia d'Ingénieurs, Université Mohammed V Agdal, BP765 Agdal, 10000 Rabat, Morocco

ARTICLE INFO

Article history:
Received 26 February 2013
Accepted 23 May 2013

Keywords:
Drought
SPI
SVI
SWI
Satellite images
Statistical analysis

ABSTRACT

Although the preliminary investigations of NDWI demonstrated its sensitivity to vegetation water content, drought indices based on NDWI short time-series are still understudied compared to those derived from NDVI and LST, such as VCI, SVI and TCI. On the basis of the open data, this paper introduces a new index derived from NDWI short time-series, and explores its performance for drought monitoring in Mediterranean semi-arid area. The new index, Standardized Water Index (SWI), was calculated and spatiotemporally compared to both meteorological drought index (TRMM-based SPI) and to agricultural drought index (NDVI-based SVI) for the hydrological years and autumn, winter and spring seasons during a period of 15 years (1998–2012). Furthermore, the response and spatial agreement of the meteorological and agricultural drought indices (SWI, SVI and SPI) were compared over two land use classes, rainfed agriculture and vegetation cover, for the studied years and seasons. The validation of SWI was based on in situ SPI and cereal productions. The analysis of the 336 cross-tables, proportions of concordance and Cohen's kappa coefficients indicate that SWI and SVI are concordant comparing to other combinations for hydrological years and for the three seasons. The study points that the spatial agreements of drought indices over rainfed agriculture and over vegetation cover are different. It is relatively more important in the rainfed agriculture than in the vegetation cover areas. Our results show that the agreement between vegetation drought indices and meteorological drought indices is moderated to low and the SPI is slightly more concordant with SWI when it is compared to SVI in autumn and winter seasons. The validation approach indicates that drought affected area, according to SWI, is highly correlated with cereal production. Likewise, a satisfactory correlation was revealed between SWI and in situ SPI.

1. Introduction

Drought is still a major hindrance to sustainable development in Morocco; its serious impacts are agricultural, socio-economical and environmental. It is a recurring phenomenon that affected all Moroccan regions with different intensities, durations and spatial extents. This is clearly proved by the reconstruction of the past droughts events and characteristics through long-term tree-rings series in Morocco for the 1000-years (Chbouki, 1992; Esper et al., 2007), and the historical documents relevant to the last centuries (Naciri, 1985). Likewise, the expectation of the Intergovernmental Panel on Climate Change (IPCC) confirms that drought and flood will be more frequent due to climate change in the Mediterranean area, including Morocco (IPCC, 2007). It is the same for Born et al. (2008), who showed that Moroccan climate tends to change toward warmer and drier conditions. As far as the historical, present and projected drought frequency is concerned, this phenomenon seems to be a structural component of Moroccan environment.

In the literature, many drought indices have been globally used in different contexts for drought characterization and monitoring. Such a variety can be explained according to the many disciplines by which they are perceived and also by the diverse sectors affected by drought. Nevertheless, the scientific community agreed that drought indices are derived into four classes, i.e. meteorological, hydrological, agricultural and socio-economical. Among widely used drought indices one can mention Palmer Drought Severity Index (PDSI) (Palmer, 1965) and Standardized Precipitation Index (SPI) (McKee et al., 1993). This latter was recommended to be used as a universal meteorological drought index according to Copenhagen declaration (WMO, 2009). SPI has several advantages, in fact, it is easy to calculate and it requires only rainfall data, additionally, it has the possibility to be implemented at different time scales and to be compared over different regions, since it is standardized. The main constraint for the operational use of the SPI is its local character. As the other in situ indices, its spatial interpolation over

* Corresponding author. Tel.: +212660599209
E-mail addresses: hichamezzine@research.emi.ac.ma, ezzine@hotmail.com (H. Ezzine), bouziane@Emi.Ac.Ma (A. Bouziane), ouazar@Emi.Ac.Ma (D. Ouazar).

0303-2434/$ – see front matter © 2013 Elsevier B.V. All rights reserved.
http://dx.doi.org/10.1016/j.jag.2013.05.005

a region or watershed requires a good density and distribution of meteorological stations (Rhee et al., 2010; Mozafari et al., 2011).

Earth observation data has overcome this constraint by providing spatial drought indices with a regular frequency. The contribution of satellite-based indices to drought characterization and spatiotemporal monitoring in different regions around the world has been well documented (Singh et al., 2003; Bhuiyan et al., 2006; Son et al., 2012; Zhang and Jia, 2013; Du et al., 2013; Wu et al., 2013), to name few. The commonly used satellite drought indices can be regrouped into four categories reflective indices, thermal indices, rainfall based indices, and their different combinations. The Normalized Difference vegetation Index (NDVI) time-series, extracted from the reflectance radiated in the near-infrared and visible red wavebands, were widely used for the calculation of several drought indices. Vegetation Condition Index, (VCI) (Kogan, 1995a,b) and Standardized Vegetation Index (SVI) (Liu and Negron-Juarez, 2001; Peters et al., 2002) are typical examples of these categories, since they were widely used for drought characterization and monitoring (Bajgiran et al., 2008; Quiring and Ganesh, 2010; Gebrehiwot et al., 2011; Du et al., 2013). The VCI is calculated in function of minimum and maximum NDVI value compiled per pixel over a time-series, whereas SVI is based on the calculation of Z scores, a deviation of the NDVI mean in units of standard deviation at the level of each pixel over a time-series. Among the examples of the used thermal drought indices, it can be cited the Temperature Condition Index (TCI) (Kogan, 1995a,b) which is calculated on the basis of maximal and minimal brightness temperature at level of pixel over a time-series. This index was implemented in different regions (Bhuiyan et al., 2006; Bayarjargal et al., 2006; Du et al., 2013).

The combination of the indices derived from near infrared, red and thermal wavebands for drought monitoring attracted the researchers interest. The Vegetation Health Index (VHI) (Kogan, 1997, 2000) is an example of this category. It is based on an additive combination of TCI and VCI. This index proves more satisfaction compared to VCI or TCI alone (Kogan et al., 2004). It was used to assess agricultural drought probability over Africa (Rojas et al., 2011). Recently, VHI has showed greater performance in detecting drought when it was evaluated by streamflow and soil moisture measurements in the Little River Experimental Watershed, Georgia, USA (Choi et al., 2013). Drought Severity Index (SDI) (Bayarjargal et al., 2006), calculated as subtraction of standardized LST and NDVI, indicated a similarity with VHI when it was compared to other reflective and thermal indices in the Mongolia's desert and desert-steppe geo-botanical zones (Bayarjargal et al., 2006). Temperature vegetation dryness index (TVDI), (calculated by parameterizing of the relationship between the NDVI and LST data), was explored in the Lower Mekong Basin. The findings showed a close agreement between TVDI and TRMM as well as a good correlation between TVDI and soil moisture (Son et al., 2012). The combination of reflective indices, thermal and precipitations ones was also examined. Brown et al. (2008) introduced a composite index, VegDRI, which integrates vegetation condition, station-based drought indices and information about land use, land cover and soils. Rhee et al. (2010) proposed a new multi-sensor drought index, called the scaled drought condition index (SDCI) which used NDVI, LST and TRMM data. The SDCI was compared to NDVI and VHI on the basis of in situ drought indices in the arid region of Arizona and New Mexico and also in the humid region of North Carolina and South Carolina. The results revealed that it is more performing (Rhee et al., 2010). Du et al. (2013) proposed a Synthesized Drought Index (SDI) based on the integration of VCI, TCI and TRMM precipitation products condition index (PCI) through principal component. It was demonstrated that SDI is highly correlated to SPI, crop yield and to drought affected area in China Shandong province (Du et al., 2013).

The potentialities of satellite near-infrared, red and thermal channels have been widely explored, through NDVI, LST and their combinations. However, the contribution of shortwave infrared (SWIR) is still in development phase and urges investigation. Normalized Difference Water Index, calculated from SWIR and Near Infrared, is known to be sensitive to vegetation water content (Gao, 1996) and may hold an important potential for drought monitoring. A quantitative analysis of bias and standard error of NDVI and NDWI, extracted from Landsat Thematic Mapper (TM) and Enhanced Thematic Mapper plus (ETM+), showed that NDWI has a superior relationship with ground-based vegetation water content measurements in Walnut Gulch Watershed (Jackson et al., 2004). Such authors suggest exploring the same approach on the basis of MODIS. NDWI values, extracted from MODIS, exhibited a quicker response to drought conditions than NDVI in Flint Hills of Kansas and Oklahoma (Gu et al., 2007). The same study showed that Normalized Difference Drought Index (NDDI), which is calculated in function of NDWI and NDVI, according to this formula ((NDVI-NDWI)/(NDVI + NDWI)), is more responsive and have wider dynamic range value than simple difference of NDVI and NDWI (Gu et al., 2007). A recent study, carried out in Sahara–Sahel transition zone, demonstrated the performance of NDWI multi-temporal series derived from Landsat-TM and ETM+ to detect permanent and seasonal water (Camposa et al., 2012). NDWI preliminary findings are encouraging, but more investigations are needed in order to explore with more details its potentialities for drought monitoring. Furthermore, NDWI time-series based drought indices is still understudied compared to those derived from NDVI and LST time-series (VCI, TCI and SVI). Throughout the literature review, it is shown that no NDWI times-series drought indices have been established till now. This line of research warrants investigation and its exploration will be initiated in this paper through a new NDWI short times-series based index.

It is confirmed that spatiotemporal comparison and correlation of satellite-based drought indices was subject of some investigations in order to evaluate drought indices compatibilities and to infer the most relevant index for decision-making. NOAA–AVHRR reflective indices (NDVI, NDVIA, SVI and VCI), thermal index (TCI) and their combinations (LST/NDVI, VH, and DSI) were compared over the desert steppe and desert geo-botanical zones of Mongolia (Bayarjargal et al., 2006). The study demonstrated that the spatial agreement of the studied indices are generally low, and the reflective indices shows higher correlation, while a lesser or no relationship is found between the thermal and combination of the thermal and reflective indices (Bayarjargal et al., 2006). A well detailed analysis of spatial and temporal drought dynamics was made during monsoon and non-monsoon seasons in the Aravalli region on the basis of VCI, TCI, VHI (extracted from NOAA-AVHRR) besides SPI and SWI (computed respectively from rain-gauge stations and wells) (Bhuiyan et al., 2006). The study found that no linear correlation exist among meteorological, hydrological, and vegetative droughts indices in the studied region, it also revealed an increase of the correlation between SPI and VCI during the monsoon season (Bhuiyan et al., 2006). VCI has been compared to five different meteorological indices, namely Palmer Drought Severity Index (PDSI), Moisture Anomaly Index (Z-index), Standard Precipitation Index (SPI), percent normal, and deciles in Texas counties (Quiring and Ganesh, 2010). It is worth noting that VCI is the most highly correlated one with the 6-month SPI, 9-month SPI and PDSI. Furthermore, the relationship between VCI and meteorological indices is significantly variable in space. Compared to counties in eastern Texas and along the Gulf Coast ($R^2 < 0.1$) (Quiring and Ganesh, 2010), the counties in northwestern and southwestern Texas have much higher correlations ($R^2 > 0.6$). Another comparison of standard and remotely sensed drought indices was conducted by Choi et al. (2013) in the Little River Experimental Watershed, Georgia, USA. It revealed that the Evaporative Stress Index (Computed from the ratio of potential and actual evapotranspiration), VHI, and PDSI had been

proven to be more performing in detecting drought in this studied region.

All those drought indices comparisons were carried out without considering the land cover/landuse classes. However, the response of drought indices can change in function of the landuse. For example, the response of agricultural drought to meteorological drought in rainfed agriculture differs from their response over area dominated by forest or by irrigated agriculture. This is the second line of research that we propose to examine.

This paper contributes to the above-mentioned two lines of research. The first one is related to the contribution of NDWI time-series based indices for drought monitoring. Hence, a new index is introduced, Standardized Water Index (SWI), derived from NDWI short time-series, it is to explore its performance for drought monitoring in Mediterranean semi-arid area. The second deeply considers the drought indices response and spatial agreement over different land cover/land use classes. Accordingly, we explored and compared the response and spatial agreement of SWI, SVI and SPI over two land cover classes (rainfed agriculture and vegetation cover). Furthermore, the study compares seasonally and annually SWI, SVI and SPI during a period of 15 years (1998–2012).

2. Study area

The study was carried out in Morocco; it is situated at the north-western part of the African continent, bordered to the north by the Mediterranean Sea, to the west by the Atlantic Ocean, to the east by Algeria, and to the south and south-east by Mauritania (Fig. 1). The total land area of Morocco is about 71.085 million hectares, including 5.8 million hectares of forests (8%), 9.2 million ha of agricultural lands (13%) and 46 million ha of pastures, rangelands and deserts. Moroccan agriculture is strongly dependent on rainfall as rainfed area represents 85% of agricultural lands (7.9 million ha). Cereal constitutes the most important crop. It is grown on a wide range of environments: oasis (area insignificant), low rainfall (arid and semi-arid, 40% area), high rainfall (sub-humid and humid, 40% area), irrigated (10% area) and mountainous area (10% area)

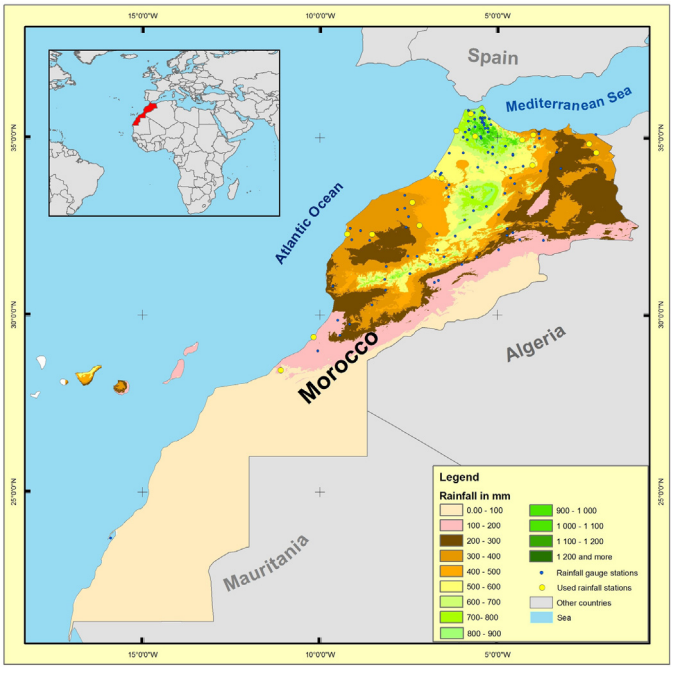

Fig. 1. Distribution of WorldClim average annual rainfall (1950–2000) and rainfall stations over the study area.

(Balaghi, 2006). The soil mosaic is so varied; it is composed mainly of entisols, vertisol, aridisols, inceptisols, alfisols, mollisols.

Morocco is essentially characterized by a Mediterranean climate, and by mild and relatively wet winters, and hot to dry summers. The climate shows enormous variations from sub-humid in the north, semi-arid to arid in the center, to Saharan in the South. It is observed that more than 50% of the precipitations are concentrated over only 15% of the country area. In addition spatial and temporal rainfall variability is considerably important. The average annual rainfalls reach more than 1000 mm in mountainous areas of the north and less than 300 mm in south. The rainy season lasts from October to March in most of the country, and December, January and February receive the maximum rainfall. The summer months have low rainfall and stormy character in general. The high inter-annual variability is also a feature of Mediterranean precipitation. The coefficient of variation (ratio of standard deviation to the mean) varies on Morocco from 30 to 40% in the west to more than 70% in the southern regions (Driouech et al., 2009). The main general circulation feature associated with rainfall variability is the North Atlantic Oscillation (NAO). Its concurrent state is inversely related to precipitations.

3. Data sets and methods

3.1. Data sets

The study is based on the processing and analysis of different sources of open data (Table 1). The datasets are composed of TRMM short time-series, SPOT Vegetation NDVI and NDWI short time series, Global Climate Data precipitation (WorldClim), and Global Land Cover. The characteristics of the used data are shown in Table 1.

The drought characterization and monitoring requires significant time-series covering a long period. However, due to data availability remote sensing researchers use relatively short time-series, which are spread over periods ranging from 10 to 18. Bayarjargal et al. (2006) used a time series of 18 years to compare drought indices derived from NOAA-AVHRR images in Mongolia. A similar time-series was used by Peter et al. (2010) to evaluate the utility of the VCI in Texas. Du et al. (2013) had recourse to MODIS and TRMM time-series of 10 years in order to calculate VCI, TCI and the synthetic drought index in Shandong province in China. A series of 12 years was used for the calculation of SVI and monitoring of drought in the United States of America (Peters et al., 2002). Wu et al. (2013) analyzed a time series of 10 years to monitor agricultural drought by the Integrated Surface Drought Index (ISDI) at the mid-eastern China. It is the same for Son et al. (2012) who treated a time-series of 10 years for monitoring drought in the Lower Mekong Basin, through the NDVI and LST derived from MODIS. A time-series of 8 years was analyzed by Choi et al. (2013), in order to compare standard and remotely sensed drought indices over the Little River Experimental Watershed, Georgia, USA.

It is worth noting that Naumann et al. (2012) have recently evaluated the uncertainties due to sample size associated with the estimation of the TRMM standardized precipitation index (SPI) and their impact on the level of confidence in drought monitoring in Africa. The study demonstrated the feasibility of using TRMM short time-series of 13 years. Its reliable drought monitoring over Africa was proved by a comparative analysis of different precipitation datasets, a studied case of Moroccan Oum Er-Rbia river basin was included (Naumann et al., 2012). In the present paper, the time-series of TRMM, NDVI and NDWI covers 15 years from 1998 to 2012. Despite being short, it includes enough variety since it covers wet years, drought years and normal years.

Table 1
Dataset used in this study.

Data	Year or period	Spatial resolution	Temporal resolution (synthesis)
TRMM precipitation (3B43)	1998–2012	0.25°	Monthly
NDVI (S10NDVI) of SPOT-Vegetation	April 1998–2012	1 km	Decadal
NDWI of SPOT-Vegetation	April 1998–2012	1 km	Decadal
Precipitation of Global Climate Data (WorldClim)	1950–2000	1 km	–
Global Land Cover of IES JRC	2000	1 km	–
Yield and Cereals production	1998–2010	–	–

The short time-series of precipitation data used in this research, from 1998 to 2012, were extracted (TRMM); it is a joined United States and Japan satellite mission. The rainfall is measured using several instruments including Precipitation Radar (PR), TRMM Microwave Image (TMI), a nine-channel passive microwave radiometer; and Visible and Infrared Scanner (VIRS), a five-channel visible/infrared radiometer (Huffman et al., 2007a,b). Among the available data, we choose the product generated by TRMM and other data sources on the basis of the 3B43 algorithm (Huffman et al., 2007a,b, 2010, 2012). This algorithm generates the precipitation rate (mm/h) at spatial resolution of 0.25 by 0.25 degree and a temporal resolution of a calendar month.

Another source of precipitation is the WorldClim Global Climate data (Hijmans et al., 2005). These data includes gridded monthly total precipitation, and monthly mean, minimum and maximum temperature, in addition to 19 derived bioclimatic variables. In this study, the average of the monthly total precipitation recoded between 1950 and 2000 was employed. It was generated through interpolation of the average monthly climate data from weather stations at a spatial resolution of 1 km by 1 km (Hijmans et al., 2005).

Normalized Difference Vegetation Index (NDVI) and Normalized Difference Water Index (NDWI) short time-series of SPOT Vegetation satellite from April 1998 to 2012 were also used in this research. The S10NDVI SPOT Vegetation products, a 10 days synthesis generated trough Maximum Value Composite (MVC), with a spatial resolution of 1 km by 1 km, were freely downloaded from SPOT Vegetation website (http://www.vgt4africa.org). The MVC algorithm selects, for a given pixel having been viewed several times, reflectance corresponding to the highest ground NDVI (Baret et al., 2006). Cloudy, bad quality or interpolated values are excluded. NDVI is calculated in function of red and near-infrared bands. It was developed by Rouse et al. (1973) and it is widely used for vegetation monitoring as well as for the calculation of agricultural drought indices, such as VCI and SVI. NDWI is a relatively a new index that was developed by Gao (1996). It is known to be sensitive to vegetation water content (Gao, 1996) due to the fact that it is calculated from Shortwave Infrared (SWIR) and Near Infrared.

The Global Land Cover 2000 and cereals production are the other open datasets used in this study. The Global Land Cover 2000 (Mayaux et al., 2003) was produced by the Institute of Environment and Sustainability. This land cover map is freely distributed in different formats (ESRI, Binary, Tiff, Img) at a spatial resolution of 1 km by 1 km (Mayaux et al., 2003). Cereals production was downloaded from the FAO Statistic website http://faostat3.fao.org/home/index.html#DOWNLOAD.

3.2. Methodological approach

3.2.1. Data processing and drought indices calculation

Monthly precipitation was computed pixel-by-pixel over the studied area on the basis of TRMM 3B43 product. The derived monthly averages during 1998–2012 were generated, and then spatially compared with WorldClim Global Climate data corresponding to the 1950–2000 period using paired comparisons and Student's t-test approach. Additionally, the regression between monthly TRMM and WorldClim averages was studied. The total seasonal precipitations for three seasons and for the hydrological years were generated using TRMM monthly precipitations for the same period. According to McKee's (1993, 1995) equations (Table 2), this dataset allowed the calculation of a monthly, seasonally and yearly probabilistic meteorological index, namely, Standardized Precipitation Index (SPI_{TRMM}).

Decadal NDVI and NDWI short time-series were processed over the same period and their monthly cumulative were calculated for the three seasons and for the hydrological years. On the basis of NDVI short time-series, the seasonal and annual Standardized Vegetation Index (SVI) were computed using the approach proposed by Peters et al. (2002). The new proposed index noted Standardized Water Index (SWI was also calculated on the basis of NDWI short time-series. SVI, SPI and SWI were based on the calculation of Z scores, $Z_{ndvi\text{-}ijk}$, Z_{p_ijk}, and Z_{ndwi_ijk}, respectively (Table2). The Z_{ndvi_ijk} is a deviation from the mean in units of standard deviation. It is calculated from the NDVI time series according to the formula proposed by Peters et al. (2002). The Z_{ndvi_ijk} was calculated for each pixel, for each season and each year, during all the period (1998–2012). Z_{p_ijk}, and Z_{ndwi_ijk} are calculated in the same way on the basis of TRMM precipitation products and NDWI, respectively. The Z scores fit the standard normal distributions with a mean of zero and standard deviation of 1. Their probability density functions are given in Table 2. To facilitate the comparison of the three indices, the same number of classes and same ranges for the three indices were adopted according to the standard classification used by McKee et al. (1993, 1995). The seven used classes are: Extreme drought (−2.00 or less), severe drought (−1.50 to −1.99), moderate drought (−1.00 to −1.49), near of normal (−0.99 to 0.99), moderately wet (1.00–1.49), severely wet (1.5–1.99) and extremely wet (2.00 or more). The three indices are standardized, the adoption of the same classes allows checking if the indices have the same deviation from their means, for each pixel, for each season or year, during the studied period (1998–2012).

The geographic distribution of the three indices (SWI, SVI and SPI_{TRMM}) was visually compared on an index-to-index, season-to-season and year-to-year basis. While intending to make the comparison and spatial analysis, the nearest neighbor resampling methodology was applied to resize the NDVI and NDWI images to a spatial resolution of 0.25 x 0.25°.

3.2.2. Indices comparison and spatial agreement assessment

In our research, the assumption made is that the response of agricultural drought indices depends on several factors, such as land cover. Hence, we attempted to compare the response of vegetation cover and rainfed agriculture land, and to assess the spatial agreement of the three indices datasets over these two land covers. Two masks were extracted from the Global Land Cover map, the first is related to vegetation land (including forest, grassland, irrigated agriculture, etc.), and the rainfed agriculture land to the second. These two masks allowed focusing on the spatial analysis at the level of vegetation cover during the first phase and at the level of rainfed agriculture land during the second phase. Furthermore, crosstabs for each combination of indices were generated on

Table 2
Satellite drought indices used in this study. NIR_{ijk}, R_{ijk} and $SWIR_{ijk}$ reflectance values at the near-infrared, red and short wave infrared wavelengths respectively, for pixel i during period j for year k. P_{ijk}, precipitation for pixel i in period j for year k; $\tilde{P}_{ij}$, multiyear average P for pixel i in period j; σP_{ij}, standard deviation of P for pixel i in period j; $NDVI_{ijk}$, $NDVI$ for pixel i in period j for year k; $\overline{NDVI}_{ij}$, multiyear average $NDVI$ for pixel i in period j; $\sigma NDVI_{ij}$, standard deviation of $NDVI$ for pixel i in period j; $NDWI_{ijk}$, $NDWI$ for pixel i in period j for year k; $\overline{NDWI}_{ii}$, multiyear average $NDWI$ for pixel i in period j; $\sigma NDWI_{ij}$, standard deviation of $NDWI$ for pixel i in period j; Z_{p_ijk}, deviation from average of precipitation in units of standard deviation for pixel i during period j for year k; Z_{ndvi_ijk}, deviation from average of $NDVI$ in units of standard deviation for pixel i during period j for year k; Z_{ndwi_ijk}, deviation from average of $NDWI$ in units of standard deviation for pixel I during period j for year k. Note that Z_{p_ijk}, Z_{p_ijk}, Z_{ndvi_ijk} and Z_{ndwi_ijk} were assumed to fit a standard normal distribution function, with 0 as mean and 1 as standard deviation. The probability distribution of Z_{p_ijk}, Z_{ndvi_ijk} and Z_{ndwi_ijk} are SPI = probability ($Z < Z_{p\_ijk}$), SVI = probability ($Z < Z_{ndvi\_ijk}$) and SWI = probability ($Z < Z_{ndwi\_ijk}$), respectively.

Symbol	Drought indices	Source	Formula
NDVI	Normalized Difference Vegetation Index	Rouse et al. (1973)	$NDVI_{ijk} = \frac{NIR_{ijk} - R_{ijk}}{NIR_{ijk} + R_{ijk}}$
NDWI	Normalized Difference Vegetation Index	Gao (1996)	$NDVI_{ijk} = \frac{NIR_{ijk} - SWIR_{ijk}}{NIR_{ijk} + SWIR_{ijk}}$
SPI	Standardized Precipitation Index	McKee et al. (1993)	$Z_{p\_ijk} = \frac{P_{ijk} - P_{ij}}{P_{\sigma ij}}$ SPI = probability ($Z < Z_{p\_ijk}$)
SVI	Standardized Vegetation Index	Peters et al. (2002)	$Z_{ndvi\_ijk} = \frac{NDVI_{ijk} - \overline{NDVI}_{ij}}{NDVI_{\sigma ij}}$ SPI = probability ($Z < Z_{ndvi\_ijk}$)
SWI	Standardized Water Index	New indices Introduced by Ezzine et al. In this paper	$Z_{ndwi\_ijk} = \frac{NDWI_{ijk} - \overline{NDWI}_{ij}}{NDWI_{\sigma ij}}$ SPI = probability ($Z < Z_{ndvi\_ijk}$)

a season-to-season, year-to-year basis and for the two land covers, the seven drought classes also were taken into consideration. Thus, the response of indices to these two land covers was examined using paired Student's *t*-test for different years and different seasons. Besides, the 336 crosstabs generated by this analysis were used to calculate the proportions of agreement between the indices and Cohen's kappa Coefficients (Table 3). By way of background, the proportion of agreement is based on pixel-by-pixel comparison which is considered as the most straightforward method of comparing two maps (Kuhnert et al., 2005). It is worth mentioning that the approach involves overlaying the maps of the two indices and on matching a pixel from the first index with the corresponding pixel in the second index and verifying if their categories fit. The proportion of agreement is then calculated as number of matched pixel divided by the total number of pixels. The proportion of agreement (P_o), sometimes labeled the proportion of observed agreement, can be easily extracted from crosstab by dividing the sum of diagonal ($\sum_{i=1}^{q} n_{ii}$) by total number of pixels (N), as shown in Table 3. The proportion of agreement has some advantages such as its simplicity to compute, easiness to understand as well as being helpful to interpret (Pontius and Millones, 2011).

Cohen's Kappa coefficient (Cohen, 1960), noted K, is widely used as statistical index not only in measuring the level of agreement between two categorized maps (Kuhnert et al., 2005; Wood, 2007), but also in evaluating the concordance of the classes of two maps by the remote sensing community (Cohen, 1960; Pontius, 1994). This coefficient is known to be more rigorous than a simple proportion of agreement since Cohen's Kappa coefficient takes into consideration the proportion of agreement due to chance P_e (or proportion of expected agreement). The standard kappa equation is indicated in Table 3. Its calculation is based on the difference between how much agreement is actually present (observed agreement) compared to how much agreement would be expected to be present by chance (expected agreement). Kappa is regarded as a measure of the difference between the observed and the expected agreement. The values can range from −1 to 1, where 1 refers to perfect agreement while 0 is exactly what would be expected by chance, and negative values indicate agreement less than chance.

In addition to the standard equation, other Kappa versions were proposed by Pontius (2000) to remedy some of its disadvantages. Pontius and Millones (2011) stressed the main Kappa criticisms, and they explained that kappa and its variance are frequently complicated to compute, difficult to understand and unhelpful to interpret. In the same paper, they proposed to use two new simpler proportions, derived from crosstab that they consider more useful than Kappa: the quantity disagreement and allocation disagreement (Pontius and Millones, 2011).

3.2.3. Validation

SWI validation was conducted in two ways, according to the approach utilized by Du et al. (2013). In the first time, SWI was compared to in situ SPI (SPI_{in}), calculated at level gauge stations. SPI_{in} is the commonly used index for meteorological drought assessment.

Table 3
Example of crosstab for two indices. The class of index 1 in columns and class of index 2 in rows. Each n_{ij} in the crosstab is the number of pixel in class i in map of index 1 and in class j in map of index 2. N_i and M_j are sums of rows and columns, respectively. P_o is the proportion of observed agreement. P_e proportion expected agreement. In our case $q = 7$.

		Map of Index 2				Total of row
		Class 1	Class 2	...	Class q	
Map of Index 1	Class 1	n_{11}	n_{12}	...	n_{1q}	$N_1 = \sum_{j=1}^{q} N_1 j$
	Class 2	n_{21}	n_{22}	...	n_{2q}	$N_2 = \sum_{j=1}^{q} N_2 j$
	...	...	...	...	...	...
	Class q	n_{q1}	n_{q2}	...	n_{qq}	$N_q = \sum_{j=1}^{q} N_q j$
		$M_1 = \sum_{j=1}^{q} N_{i1}$	$M_2 = \sum_{j=1}^{q} N_{i2}$	...	$M_q = \sum_{j=1}^{q} N_{iq}$	N

(1) $K = \frac{P_o - P_e}{1 - P_e}$;
(2) $P_o = \frac{1}{N} \sum_{i=1}^{q} n_{ii}$;
(3) $P_e = \frac{1}{N^2} \sum_{i=1}^{q} M_i N_i$.

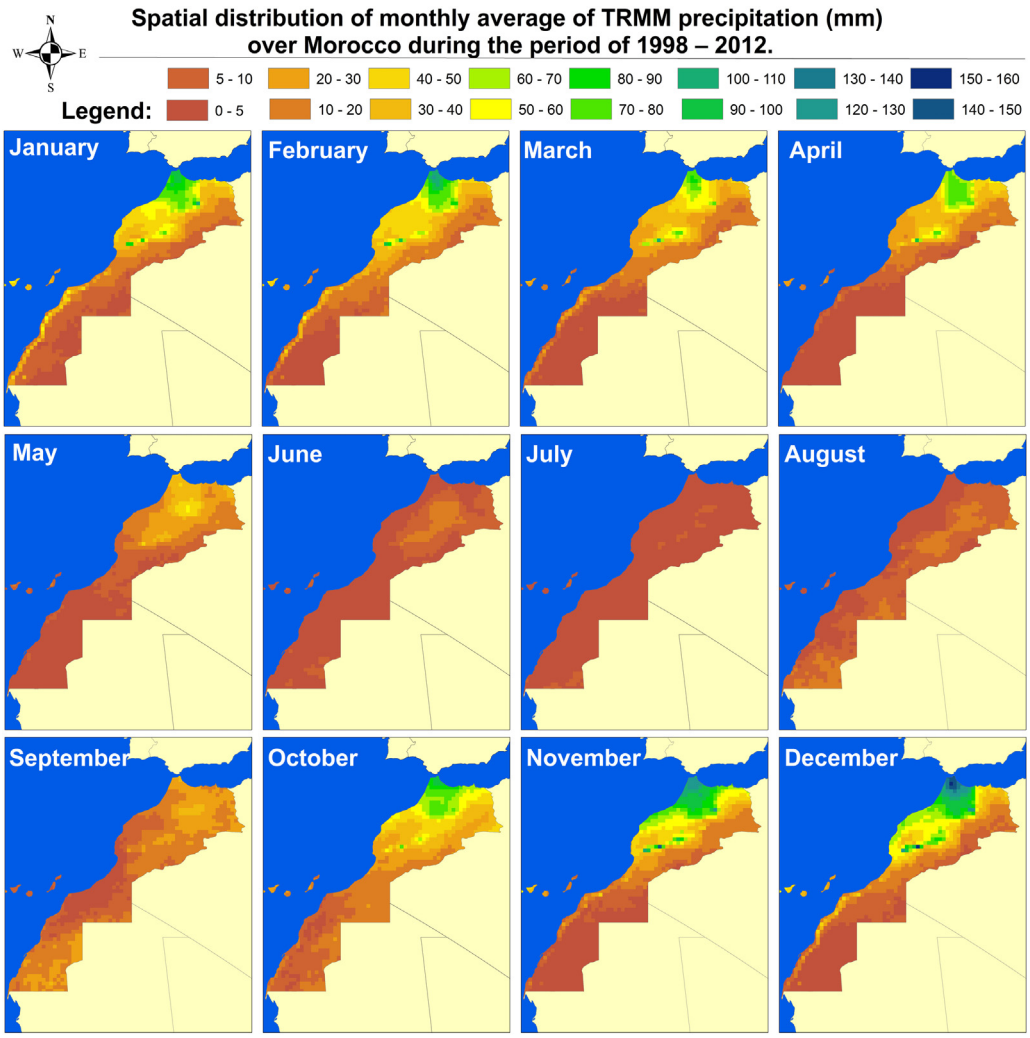

Fig. 2. Spatial distribution of monthly average of TRMM precipitation products products over Morocco during the period of 1998–2012.

Secondly, SWI was validated on the basis of cereal production, which is a good proxy for agricultural drought.

Indeed, rainfall data recorded in sixteen well-distributed weather stations, covering different periods while overlapping over 1977–2012, were used to calculate the SPI_{in} for all the studied seasons (autumn, winter and spring). Then, the correlation between the in situ SPI_{in} and SPI_{TRMM} was determined at level of corresponding pixel.

The analyzed period in this article ranges from 2004 to 2007. This period was chosen because it includes a dry year, a wet year and an intermediate year, and due to the absence of any significant hazards (floods, locusts, etc.). It should be noted that although the number of stations is relatively low (16), it can be informative about the validation of the approach. A total of 15 stations were used by Du et al. (2013) in Shandon to validate the SDI. Duan and Bastiaanssen (2013) have used eight meteorological stations to validate the downscaling approach of TRMM 3B43 products at Lake Tana Basin located in North West Ethiopia.

The relevance of SWI in terms of agricultural drought monitoring was evaluated through the correlation between the areas affected by drought according to SWI, and cereal production. A similar method was adopted by Du et al. (2013) to validate the drought synthetic index using 11 observations. In this work, the number of observations is 13 years from 1999 to 2011. Their corresponding cereal productions were acquired from the FAO website. Hence, the annual SWI were calculated for the studied agricultural companions. Then the drought-affected areas, according to SWI, were calculated at an annual basis to study their correlation with cereal productions. The same approach has been adopted to study the correlation between cereal production and SVI and SPI_{TRMM}.

4. Results and discussion

4.1. Spatiotemporal distribution and comparison of TRMM and WorldClim rainfall

The visual analysis of TRMM rainfall spatial distribution over Morocco shows spatiotemporal variability depending on the season as well as the proximity of the sea and the altitude as depicted in Fig. 2. In general, the north-west is wetter than the rest of the country. The rainfall during the winter and spring can reach an average of 60–150 mm per month in this region. The rainfall decreases gradually from north to south and south-east, and it is limited to less than 10 mm per month. The summer rainfall is very low, it is generally less than 5 mm during the months of June, July and August. The overall distribution of TRMM rainfall shows a good agreement with the well-known pattern and rainfall cycle in Morocco.

The pixel-to-pixel comparison of the monthly TRMM average during 1998–2012 and WorldClim average for the year of 1950–2000 demonstrated that the maximum differences were

Table 4
Paired means comparison and pixel-to-pixel regression parameters of TRMM-precipitations (1998–2012) and WorldClim precipitations (1950–2000).

Months	Paired comparison parameters		Regression parameters	
	Average difference	Observed student-*t*	*R*-squared	Regression equation
January	−3.410***	−7.935	0.81***	$P_{trmm} = 4.19 + 0.72\,P_{wc}$
February	−1.360***	−3.392	0.84***	$P_{trmm} = 5.37 + 0.74\,P_{wc}$
March	−7.720***	−14.330	0.78***	$P_{trmm} = 4.45 + 0.55\,P_{wc}$
April	−4.022***	−10.750	0.79***	$P_{trmm} = 1.45 + 0.76\,P_{wc}$
May	−1.040***	−5.216	0.85***	$P_{trmm} = 2.39 + 0.75\,P_{wc}$
June	−0.750***	−5.720	0.59***	$P_{trmm} = 2.18 + 0.45\,P_{wc}$
July	−0.199***	−3.312	0.41***	$P_{trmm} = 1.10 + 0.41\,P_{wc}$
August	3.335***	34.880	0.43***	$P_{trmm} = 1.45 + 0.71\,P_{wc}$
September	3.270***	16.744	0.43***	$P_{trmm} = 6.91 + 0.69\,P_{wc}$
October	7.270***	21.724	0.77***	$P_{trmm} = 6.1 + 1.06\,P_{wc}$
November	−2.940***	−6.300	0.78***	$P_{trmm} = -2.16 + 0.97\,P_{wc}$
December	−4.607***	−10.274	0.84***	$P_{trmm} = -1.94 + 0.92\,P_{wc}$

*** Significant at 0.01 probability level.

recorded during the month of March (−7.7 mm) and October (7.2 mm). These months can record an average exceeding 100 mm in some areas. For the other months, the average difference varied from −4.2 to 3 mm. Overall, the average of TRMM precipitation products are less than the average of WorldClim precipitations except in the end of summer season (August) and in the beginning of autumn season (September and October). These findings are compatible with the underestimations of rainfall in the wet season and overestimation in the dry season in Saudi Arabia (Almazroui, 2011) and Bangladesh (Islam and Uyeda, 2007) despite the fact that the months are different for the wet and dry seasons, and TRMM was compared to gauge stations. This difference, even being small in our case, can be explained by a combination of several factors such as spatial interpolation of gauge measurements for WorldClim data, the loss of information due to resampling of TRMM measurements, and the changes in rainfall patterns between the two periods. The available data did not allow discriminating between the parts of different errors.

The analysis of pixel-to-pixel paired regression between the average monthly TRMM and WorldClim precipitations shows a high and significant correlation according to Student's *t*-test, as indicated in the Table 4. The correlation coefficients range from 0.64 to 0.92. The lowest correlation coefficients correspond to summer season where correlation coefficients of 0.64, 0.65 and 0.65 were obtained respectively in July, August and September. Since the difference between the TRMM data covering the period 1998–2012 and WorldClim covering the period 1950–2000 is weak, and their correlation is highly significant. We can consider that the period 1998–2012 is a representative sample.

4.2. Interpretation of SPI, SVI and SWI maps

According to the SPI_{TRMM} maps (Fig. 3), moderate meteorological drought was recorded in different regions, with different extents during 1998–1999, 1999–2000, 2000–2001, and 2002–2003. The hydrological years 2004–2005, 2006–2007 and 2007–2008 have experienced moderate and severe meteorological drought in some limited areas. Humid and extreme humid conditions were widely observed over 2008–2009, 2009–2010 and 2010–2011.

With regard to agricultural drought that was assessed by SVI and SWI, severe and extreme drought were recorded in different regions, with different extents during all the studied period, except for the years 2008–2009, 2009–2010 and 2010–2011. In these years, the SVI and SWI showed higher values indicating a good and very good vegetation conditions. In general, maps of different indices have more or less the same trend and are consistent with droughts recorded in Morocco. One example can be cited here; the droughts of 1999 and 2007 appear in the Maps. It is the same for the extremely wet areas identified in 2009 and 2010 by SPI_{TRMM}, which is consistent with the food occurred in the region of Gharb (Northwestern Morocco), after heavy rainfall.

In term of areas, SPI_{TRMM}, SVI and SWI categories vary approximately in the same sense, as it is illustrated by Fig. 4. The years characterized by good cereals production coincide with significant area of good and very good vegetation condition; such was the case for the years 2002–2003, 2003–2004, 2005–2006, 2008–2009 and 2009–2010. During these years, according to FAO database, sums of cereals production were 7,973,669, 8,602,501, 9,241,617, 10,443,598 and 7,834,390 tons respectively. Such low cereals productions were recorded during the years while SPI_{TRMM}, SVI and SWI show significant area of moderate, severe and extreme drought. According to the same source, the sums of cereals production were 3,842,646, 1,995,870 and 2,505,132 tons in 1998–1999, 1999–2000, and 2006–2007, respectively.

Fig. 5 shows spatiotemporal monitoring of drought in Morocco over three seasons (autumn, winter and spring) on the basis of meteorological (SPI_{TRMM}) and agricultural indices (SVI and SWI). The seasonal monitoring experiences more spatiotemporal variability than the annual for the three indices. What to be noticed is that drought appears randomly in different seasons. The extent and the intensity of drought can change from season to season. It seems that this variability can be hidden when drought is monitored at annual temporal scale since rainfall, NDVI and NDWI are aggregated. However, this does not allow apprehending drought across seasons. Similar point was noticed over monsoon and non-monsoon seasons in the Aravalli terrain of Rajasthan province of India (Bhuiyan et al., 2006). It is worth monitoring this phenomenon at a quarter basis in order to detect eventual seasonal drought while considering the impact of drought on vegetation last three months in the subhumid and semi-arid areas (Udelhoven et al., 2009).

4.3. Spatial agreement of drought indices

Beyond a visual comparison of the three indices and their areas, we are interested in a rigorous evaluation, pixel-by-pixel, of the spatial agreement of three indices to better assess their compatibility and their response.

In this sense, the spatial agreements of the three indices over seasonal and annual scales were analyzed on the basis of the proportion of agreements and Cohen's kappa coefficients. The latter were generated for all the possible combinations through crosstabs. An example of the 336 crosstabs generated in this study is provided in Table 5. In this case, while considering the seven

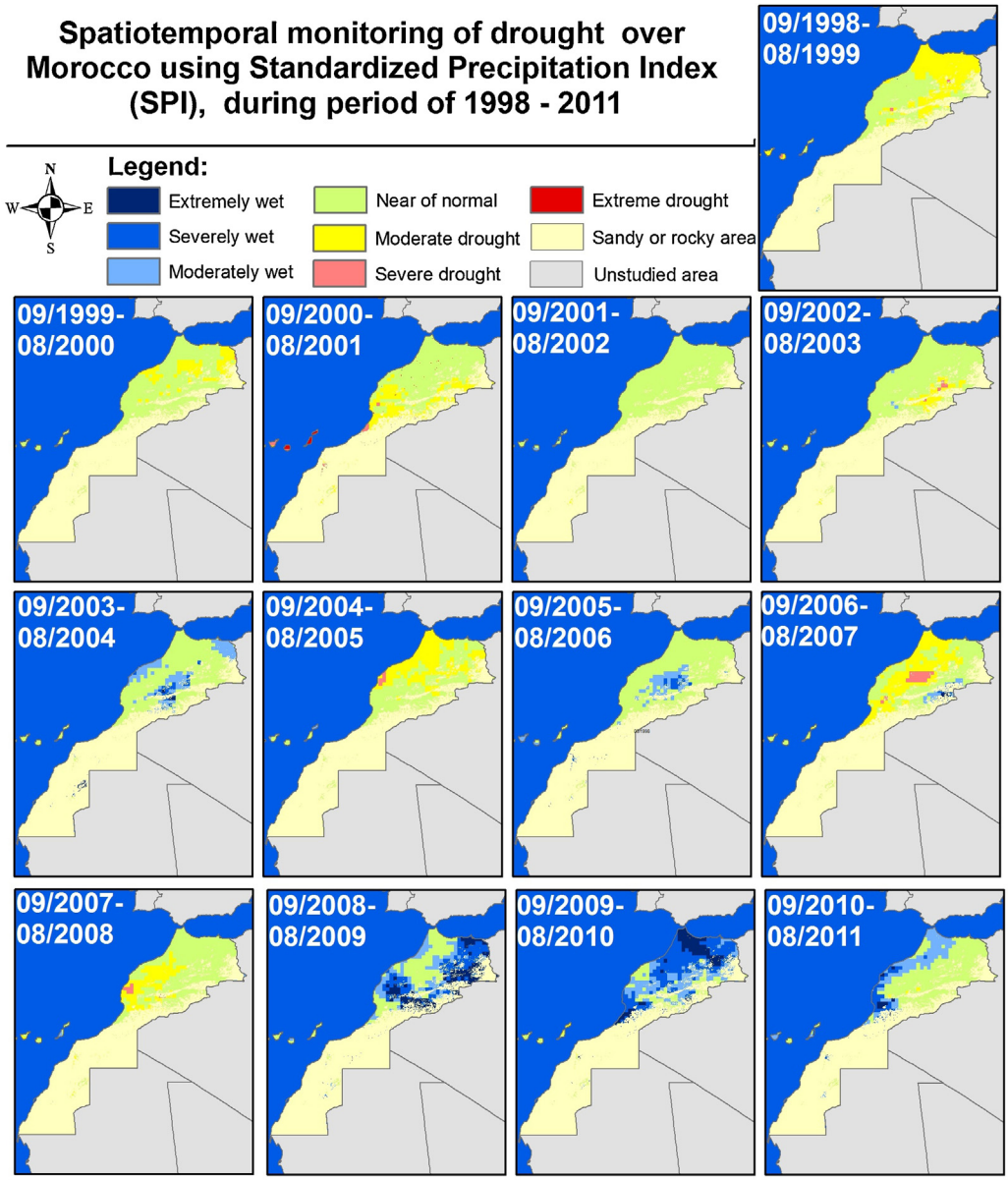

Fig. 3. Spatiotemporal monitoring of drought using SPI, 1998–2012.

drought categories, the proportion of agreement between SVI and SWI for the year 2003 is 77%. This means that 77% of the pixels were assigned to the same category of drought by the two indices (SVI and SWI).

Fig. 6 shows the proportion of agreement recorded for different combinations and their associated Kappa Cohen's coefficients. The figure reveals that the proportion of agreements can vary from 0.00 until 0.94, indicating a very low and very high agreement, respectively. The proportion of agreement varies on a year-to-year, season-to-season, and index-to-index basis. The Kappa Cohen's coefficient varies also in the same way.

In general, the proportions of spatial agreement between vegetation drought indices (SVI and SWI) are higher than the proportion of agreement between meteorological (SPI_{TRMM}) and vegetation

Table 5
Example of crosstab of SVI and SWI for the year 2003.

		SVI						
		E. humide	T. humide	M. humide	P. normale	M. sèche	S. sèche	E. sèche
SWI	E. humide	0.05	0.94	0.23	0.01	0.00	0.00	0.00
	T. humide	0.02	1.40	3.55	0.37	0.00	0.00	0.00
	M. humide	0.02	0.73	12.69	7.64	0.00	0.00	0.00
	P. normale	0.03	0.30	5.87	62.68	0.33	0.02	0.00
	M. sèche	0.00	0.00	0.00	2.74	0.22	0.00	0.00
	S. sèche	0.00	0.00	0.00	0.10	0.03	0.00	0.00
	E. sèche	0	0	0	0.00	0.00	0	0

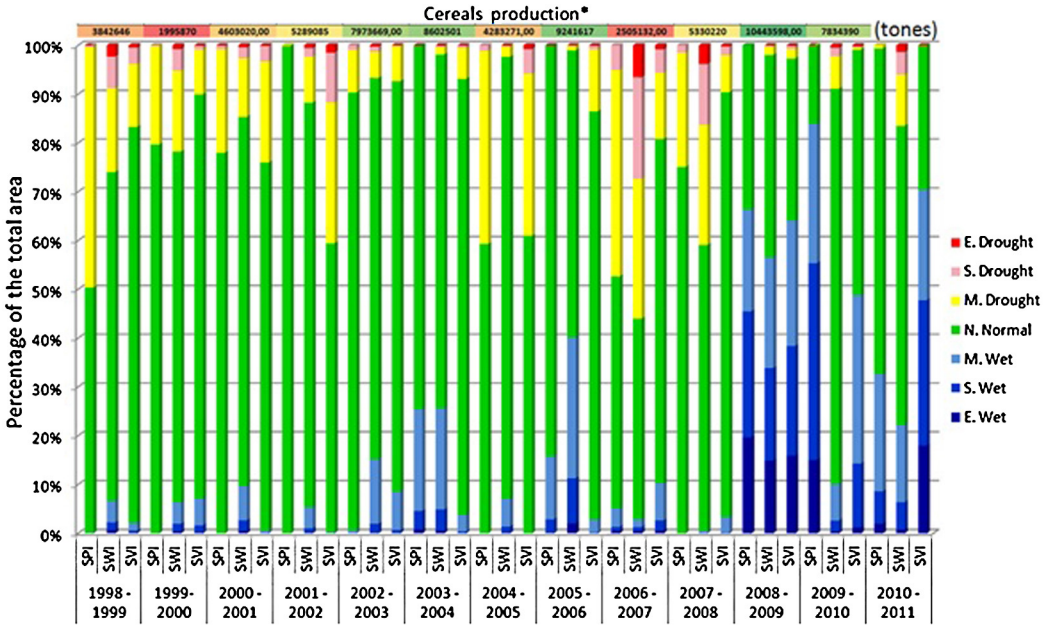

Fig. 4. Percentage of total area of drought indices categories and yield production between 1998 and 2012.

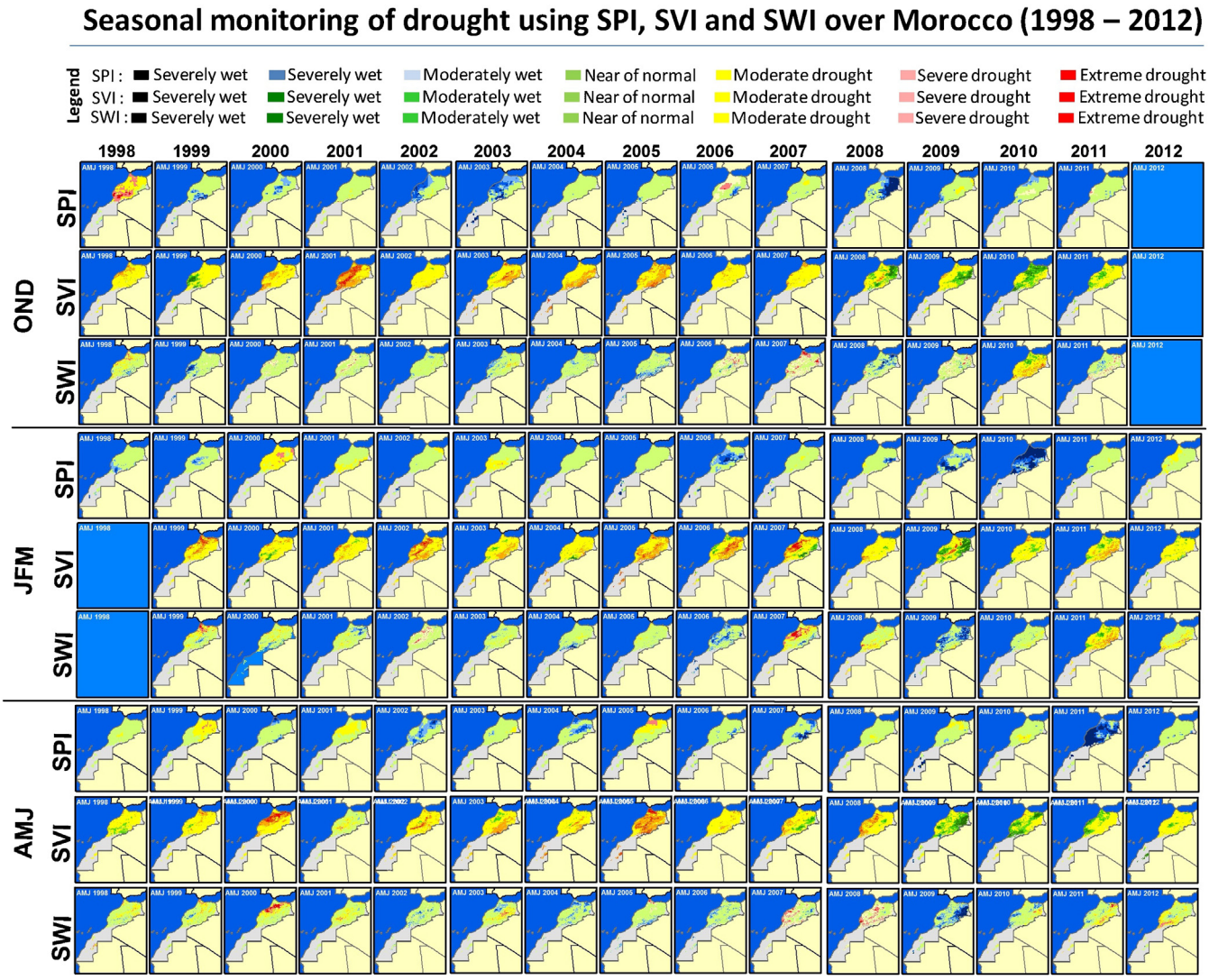

Fig. 5. Seasonal monitoring of drought using SPI, SVI and SWI indices over Morocco.

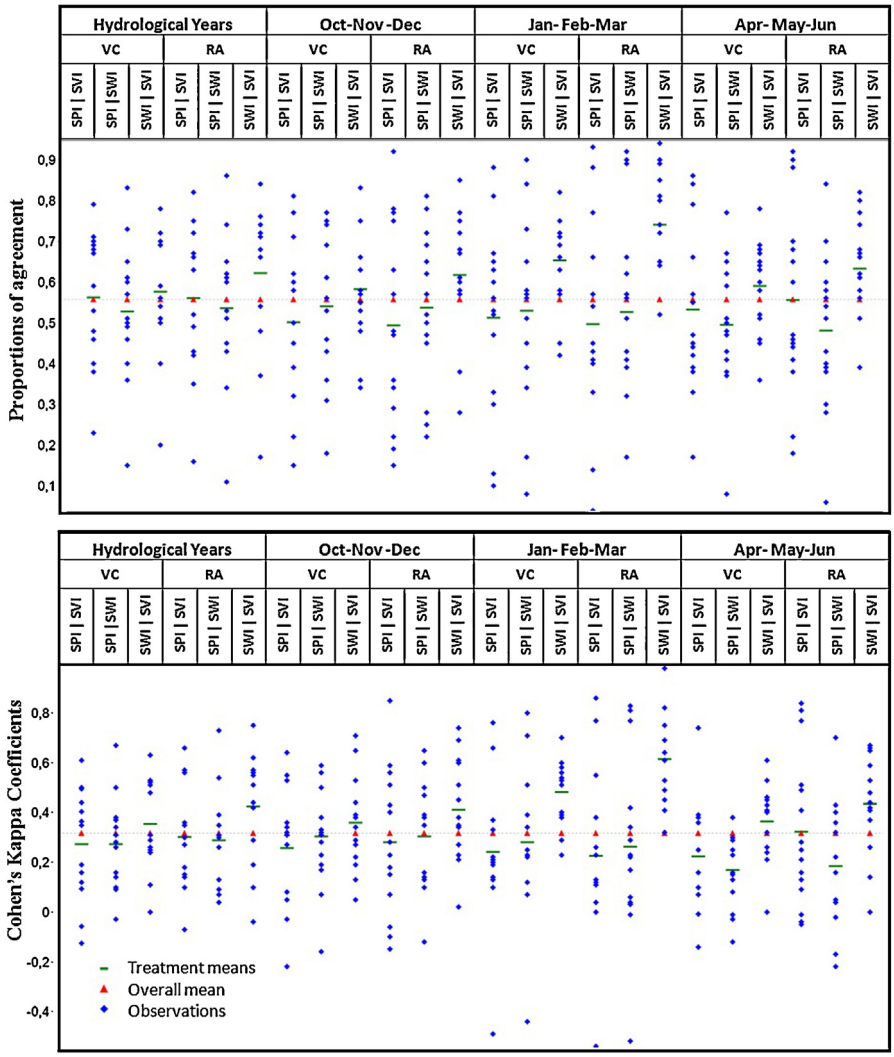

Fig. 6. Proportions of agreement and Cohen's Kappa coefficients of SPI, SVI and SWI over hydrological years and autumn, winter, spring seasons at level of rainfed agriculture (RA) and vegetation cover (VC).

drought indices. The maximum of agreement is observed during the winter season. This seems to be normal since it is at the same time a rainy and vegetation growing season, so there is significant response between meteorological conditions and vegetation growing. The kappa coefficients have the same tendency as proportions of agreement. These coefficients are more significant for SVI and SWI combinations comparing to SPI and SVI, and to SPI_{TRMM} and SWI.

The proportions of spatial agreement between vegetation drought indices and meteorological drought index are partial and vary from moderate to low. Indeed, it appears that meteorological drought, indicated by SPI, does not correspond necessarily to agricultural drought observed by SVI and SWI. Likewise, comfortable meteorological conditions expressed by high value of SPI can correspond to agricultural drought. Similar results were found by Bhuiyan et al. (2006) in the Aravalli region, and in the Mongolia's desert and desert-steppe geo-botanical zones by Bayarjargal et al. (2006). This finding can be explained by the temporal distribution of rainfall. Indeed, a very high SPI value (extremely humid or humid) does not mean good temporal distribution of rainfall during the season. This can interfere with normal vegetation growing, and thus results in low or moderate SVI values. Similarly, although low or moderate rainfall indicates a low SPI, they can be temporally well distributed over the vegetation growing cycle. Thus, result in higher values of SVI and SWI. On the other hand, the soil depth and its holding capacity is another parameter to be considered in the interpretation of meteorological and agricultural drought.

Fig. 6 reveals also that SWI is slightly more concordant with SPI_{TRMM} than SVI during autumn and winter seasons. Most of the rainfall is recorded during these two rainy seasons, so it seems logical that the SWI is relatively better correlated with SPI. This is because it is calculated from the NDWI known by its sensitivity to water and by its correlation to soil moisture as shown by Gu et al. (2008).

Through the analysis of the 339 crosstab, the proportions of agreement and kappa coefficients seem to be redundant since the two statistics bring the same information. These results confirm the recent finding of Ponitus et al. (2011).

4.4. Comparison of spatial agreement over rainfed agriculture and vegetation cover

One of the questions to be explored here is whether there is a difference or not between the responses of agricultural drought to meteorological drought in different land uses. In this paper we consider two landuse classes: rainfed agriculture and vegetation covers (including forest, pasture, irrigated agriculture, etc.).

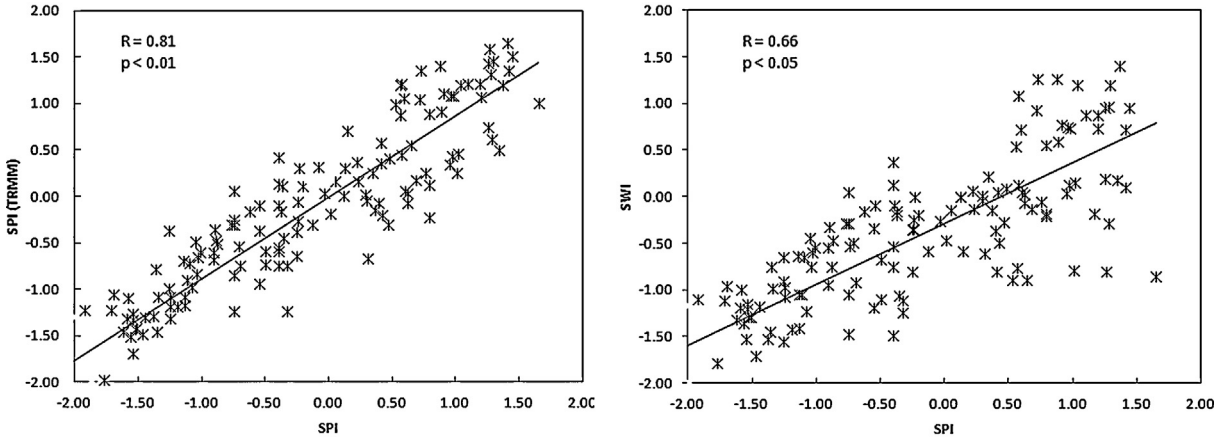

Fig. 7. Scatter plots and correlation coefficient *R* values betweens seasonal SPI (gauge stations), SPI (TRMM) and SWI (SPOT Vegetation) for the years 2004–2007.

The analysis of the spatial agreements between drought indices over vegetation cover (forest, grassland, irrigated agriculture, etc.) and rainfed agricultural land revealed that there is a difference in the proportions of agreement (Fig. 5). The overall agreement over rainfed agriculture land is relatively more important than over vegetation cover, especially for the case of SVI and SWI combinations, for both seasonal and annual periods. The difference in the proportion of agreement can reach an average of 9% of the total area for the case of SVI and SWI during winter season, with a high level of signification according to Student's *t*-test at 95% confidence interval. A difference of 4% was also noted for the proportion of agreement between the two indices during spring season, with the same level of statistical signification. On the basis of this finding, it is suggested to take into consideration land use in the interpretation of drought indices and in their comparisons. This relative high agreement implies that response of vegetation drought indices to meteorological drought is relatively better over rainfed agriculture. This can be explained by the fact that roots system is less developed in the rainfed crops comparing to forests that have a developed and deep root system. Thus, it has more access to water resources in the case of light drought. Furthermore, it can be highlighted by the fact that irrigated agriculture can have a water supply in the case of absence of severe hydrological drought, so that the response of vegetation drought indices to meteorological drought is less important over irrigated area.

4.5. Validation of SWI

In addition to its spatiotemporal comparison with SPI_{TRMM} through the proportions of agreement and Cohen's kappa coefficient, the relevance of SWI was also based on the in situ SPI. Fig. 7 shows the result of the correlation between SWI and in situ SPI. It pointed out that these two indices are significantly correlated. The same figure shows a strong correlation between the SPI_{in} and SPI_{TRMM}. The later and SWI can be used for relevant meteorological drought monitoring while offering the advantage of being spatial.

The correlation between the annual cereal production and drought affected area, according to SWI, SVI and SPI_{TRMM}, was analyzed to assess the relevance of SWI in monitoring agricultural drought, and to compare it with the two other indices (SVI and SPI_{TRMM}). The results of this analysis are illustrated in Fig. 8. It shows a negative significant correlation ($R = -0.83$) between the surfaces affected by drought according to SWI and cereal production. This correlation is slightly less than the correlation obtained with the SVI ($R = -0.88$), and at the same time it is greater than the correlation obtained by SPI ($R = -0.60$). This result demonstrates sufficient relevance of SWI for spatial monitoring of agricultural drought, in addition to SVI which is widely used. It should be noted that the number of samples used for this validation is relatively low (13 years). A sample with similar size was used to validate the SDI by Du et al. (2013).

The relatively lower correlation between SPI_{TRMM} and cereal production can be explained by the fact that it depends not only on rainfall amounts, but also on their temporal distribution through vegetation growing stages.

For the case of SVI and SWI, the same figure reveals that the small areas affected by drought are not sufficient to explain an important cereal production. This is quite logical since it is the areas of the favorable conditions (high SVI and SWI) that can explain this production.

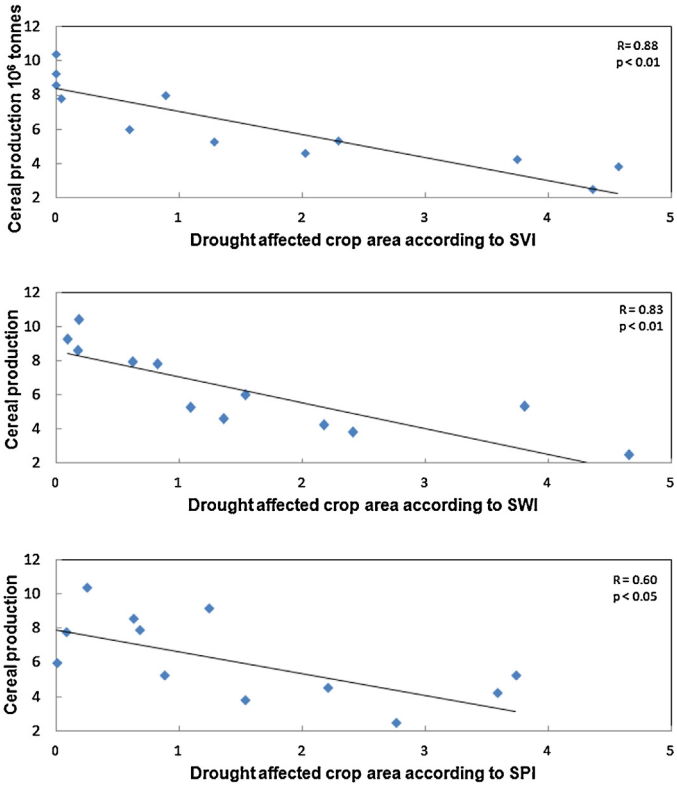

Fig. 8. Scatter plots and correlation coefficient of *R* values between droughts affected crop area (10^6 h m^2) according to annual SVI, SWI and SPI and total cereal production (109 kg) from 1999 to 2011.

4.6. Study limitation

The study was based on standardized drought indices (normalized on the basis of the standard deviation) that provide the ability to compare different regions. Thus it may be extended to other zones taking into account the following limitations:

- The indices were generated and compared to a quarterly time scale, it is considered sufficient to have a good vegetation response to rainfall in the subhumid and semiarid area. Other time scales might be more appropriate in other regions, for the comparison purpose. Overall, SWI can be calculated at a decadal time scale, such as SVI, or monthly scale, like SPI. However, the comparison of the three indices to these temporal scales may be irrelevant since the interaction of precipitation and vegetation cover in short period is not sufficiently documented.
- The used NDVI and NDWI decadal synthesis were generated through MVC algorithm. In the cloudy regions, before reproducing this study, further cleaning can be required in order to remove remaining cloud effects. Otherwise, the possible decrease of NIR radiance (Hird and McDermid, 2009) can influence the indices values.
- The used drought indices in this paper are meteorological and agricultural. They can be applied to the drought monitoring in the areas dominated by rainfed agriculture where extensive cultural practices are used. The integration of a hydrological drought index may be relevant for irrigated agricultural areas. Similarly, when interpreting these indices, it is important to consider the cultural practices such as the fertilization in intensive farming areas.
- The sample size used for SWI validation is relatively small (16 stations). For a better appreciation of this index, it is strongly recommended to consider more stations. In this respect, it will be relevant to integrate soil moisture data in the validation process.
- The evaluation of spatial agreement between meteorological and agricultural drought indices was based on the proportion of agreement and Kappa coefficient. The latter was criticized by some authors who recommend two new proportions: the quantity disagreement and allocation disagreement (Pontius and Millones, 2011).

5. Conclusion

The study introduced a new NDWI – short time-series based drought index, Standardized Water Index, and conducted a seasonal comparison between remotely sensed meteorological and agricultural drought indices over rainfed agriculture and vegetation cover zones of Morocco during 1998–2012 period.

The comparison of the monthly averages of TRMM precipitation products over the period 1998–2012 and the monthly average of WorldClim precipitations recorded for the period 1950–2000, shows a slight difference. This difference varies from one month to another and it never exceeds 7.7 mm. This was observed during the month of March where the monthly precipitations can reach an average of more than 100 mm. The pixel-to-pixel regression shows a high level of correlation between the two precipitation datasets besides an important level of signification, at a confidence interval of 95% over all the months.

The spatiotemporal monitoring of drought concludes that drought can occur randomly in different regions in Morocco over the three seasons, autumn, winter and spring and at the annual scale.

Through the analysis of spatial agreement of drought indices, it was shown that the agricultural drought indices, namely SVI and SWI are more concordant. The spatial agreement between meteorological and agricultural drought indices was partial. Compared to SVI during autumn and winter seasons, SWI seems to be slightly more concordant with SPI_{TRMM}.

The spatial agreement of meteorological and agricultural drought indices over rainfed agriculture is slightly more important than over the vegetation cover. A significant difference of 9% was recorded during winter season. This agreement can be explained by the fact that roots system are less developed in the rainfed crops compared to forests that have a developed and deep root system. Hence, it has more access to water resources in the case of slight drought. This can be explained by the fact that irrigated agriculture can have water supply in the case of absence of severe hydrological drought. It is strongly recommended to take into account land use in the studies related to drought indices comparisons and correlations. The validation of SWI by its comparison with in situ SPI showed a significant correlation. A high correlation was also observed between SWI drought affected area and cereal production.

The study was based on the freely available short-time series data, mainly TRMM precipitation products, SPOT Vegetation – NDVI and NDWI. It demonstrated how to overcome the lack of data for drought characterization and monitoring in some developing countries, where data are unavailable or its access is still difficult or very expensive.

Further investigations are required in order to establish a comprehensive early warning and drought monitoring system or a spatial drought dashboard. This can be reached by integrating thermal time-series data and soil moisture parameters that it can be linked to a model.

References

Almazroui, M., 2011. Calibration of TRMM rainfall climatology over Saudi Arabia during 1998–2009. Atmospheric Research 99 (2011), 400–414.

Bajgiran, P.R., Darvishsefat, A.A., Khalili, A., Makhdoum, M.F., 2008. Using AVHRR-based vegetation indices for drought monitoring in the Northwest of Iran. Journal of Arid Environments 72 (June (6)), 1086–1096.

Balaghi, R., 2006. Wheat grain yield forecasting models for food security in Morocco. University de Liege, pp. 116 (Ph.D thesis).

Baret, F., Bartholomé, E., Bicheron, P., Borstlap, G., Bydekerke, L., Ombal, B., Derwae, J., Geiger, B., Gontier, E., Grégoire, J.M., Hagolle, O., Jacobs, T., Leroy, M., Piccard, I., Samain, O., Van Roey, T., 2006. VGT4Africa User Manual., pp. 268.

Bayarjargal, Y., Karnieli, A., Bayasgalan, M., Khudulmur, S., Gandush, C., Tucker, C.J., 2006. A comparative study of NOAA–AVHRR derived drought indices using change vector analysis. Remote Sensing of Environment 105, 9–22.

Bhuiyan, C., Singh, R.P., Kogan, F.N., 2006. Monitoring drought dynamics in the Aravalli region (India) using different indices based on ground and remote sensing data International Journal of Applied Earth Observation and Geoinformation 8, 289–302.

Born, K., Christoph, M., Fink, A.H., Knippertz, P., Paeth, H., Steph, P., 2008. Moroccan climate in present and future: combined view from observational data and regional climate scenarios. In: Zeini, F., Hötzl, H. (Eds.), Climatic Changes and Water Resources in the Middle East and North Africa. Springer, pp. 29–45.

Brown, J.F., Wardlow, B.D., Tadesse, T., Hayes, M.J., Reed, B.C., 2008. The Vegetation Drought Response Index (VegDRI): a new integrated approach for monitoring drought stress in vegetation. GIScience & Remote Sensing 45, 16–46.

Camposa, J.C., Sillerob, N., Britoa, J.C., 2012. Normalized difference water indexes have dissimilar performances in detecting seasonal and permanent water in the Sahara–Sahel transition zone. Journal of Hydrology 464–465, 438–446, 25 September.

Chbouki, N., 1992. Spatiotemporal characteristics of drought as inferred from tree-ring data in Morocco. The University of Arisona, Department of Geosciences, USA (Ph.D thesis).

Choi, M., Jacobs, J.M., Anderson, M.C., Bosch, D.D., 2013. Evaluation of drought indices via remotely sensed data with hydrological variables. Journal of Hydrology 476 (January (7)), 265–273.

Cohen, J., 1960. A coefficient of agreement for nominal scales. Educational and Psychological Measurement 20, 27–46.

Driouech, F., Déqué, M., Mokssit, A., 2009. Numerical simulation of the probability distribution function of precipitation over Morocco. Climate Dynamics 32, 1055–1063, http://dx.doi.org/10.1007/s00382-008-04310-6.

Du, L., Qingjiu, T., Tao, Y., Qingyan, M., Tamas, J., Peter, U., Yan, H., 2013. A comprehensive drought monitoring method integrating MODIS and TRMM data. International Journal of Applied Earth Observation and Geoinformation 23, 245–253, August.

Duan, Z., Bastiaanssen, W.G.M., 2013. First results from Version 7 TRMM 3B43 precipitation product in combination with a new downscaling-calibration procedure. Remote Sensing of Environment 131, 1–13.

Esper, J., Franck, D., Büntgen, U., Verstege, A., Luterbacher, J., Xoplaki, E., 2007. Long-term drought severity variations in Morocco. Geophysical Research Letters 34, L17702, http://dx.doi.org/10.1029/2007GL030844.

Gao, B.C., 1996. NDWI—a normalized difference water index for remote sensing of vegetation liquid water from space. Remote Sensing of Environment 58 (3), 257–266.

Gebrehiwot, T., Veen, A.V.D., Maathuis, B., 2011. Spatial and temporal assessment of drought in the Northern highlands of Ethiopia. International Journal of Applied Earth Observation and Geoinformation 13 (June (3)), 309–321.

Gu, Y., Brown, J.F., Verdin, J.P., Wardlow, B., 2007. A five-year analysis of MODIS NDVI and NDWI for grassland drought assessment over the central Great Plains of the United States. Geophysical Research Letters 34, L06407, http://dx.doi.org/10.1029/2006GL029127.

Gu, Y., Hunt, E., Wardlow, B., Basara, J.B., Brown, J.F., Verdin, J.P., 2008. Evaluation of MODIS NDVI and NDWI for vegetation drought monitoring using Oklahoma Mesonet soil moisture data. Geophysical Research Letters 35, L22401, http://dx.doi.org/10.1029/2008GL035772.

Hijmans, R.J., Cameron, S.E., Parra, J.L., Jones, P.G., Jarvis, A., 2005. Very high resolution interpolated climate surfaces for global land areas. International Journal of Climatology 25, 1965–1978.

Hird, J.N., McDermid, G.J., 2009. Noise reduction of NDVI time series: an empirical comparison of selected techniques. Remote Sensing of Environment 113, 248–258.

Huffman, G.J., Adler, R.F., Bolvin, D.T., Gu, G., Nelkin, E.J., Bowman, K.P., Hong, Y., Stocker, E.F., Wolff, D.B., 2007a. The TRMM multi-satellite precipitation analysis: QuasiGlobal, multi-year, combined-sensor precipitation estimates at fine scale. Journal of Hydrometeorology 8 (1), 38–55 ftp://meso.gsfc.nasa.gov/agnes/huffman/papers/TMPA_jhm_07.pdf.gz.

Huffman, G.J., Adler, R.F., Bolvin, D.T., Nelkin, E.J., 2010. In: Hossain, F., Gebremichael, M. (Eds.), The TRMM Multi-satellite Precipitation Analysis (TMPA). Chapter 1 in Satellite Rainfall Applications for Surface Hydrology. Springer Verlag, pp. 3–22, ISBN: 978-90-481-2914-0.

Huffman, G.J., Adler, R.F., Curtis, S., Bolvin, D.T., Nelkin, E.J., 2007b. In: Levizzani, V., Bauer, P., Turk, F.J. (Eds.), Global Rainfall Analyses at Monthly and 3-hr Time Scales. Chapter 23 of Measuring Precipitation from Space: EURAINSAT and the Future. Springer Verlag (Kluwer Academic Pub. B.V.), Dordrecht, The Netherlands, pp. 291–306.

Huffman, G.J., Stocker, E.F., Bolvin, D.T., Nelkin, E.J., Adler, R.F., 2012. Last updated 2012: TRMM Version 7 3B42 and 3B43 Data Sets. NASA/GSFC, Greenbelt, MD http://mirador.gsfc.nasa.gov/cgibin/mirador/presentNavigation.pl?tree=project&project=TRMM&dataGroup=Gridded&CGISESSID=5d12e2ffa38ca2aac6262202a79d882a

IPCC, 2007. In: Solomon, S., Qin, D., Manning, M., Chen, Z., Marquis, M., Averyt, K.B., Tignor, M., Miller, H.L. (Eds.), The Physical Science Basis. Contribution of Working Group I to the Fourth Assessment Report of the Intergovernmental Panel on Climate Change. Cambridge University Press, Cambridge, United Kingdom/New York, NY, USA, p. 996.

Islam, M.N., Uyeda, H., 2007. Use of TRMM in determining the climatic characteristics of rainfall over Bangladesh. Remote Sensing of Environment 108, 264–276.

Jackson, T.J., Cosh, D.C.M., Li, F., Anderson, M., Walthall, C., Doriaswamy, P., Hunt, E.R., 2004. Vegetation water content mapping using Landsat data derived normalized difference water index for corn and soybeans. Remote Sensing of Environment 92 (4), 475–482, 30 September.

Kogan, F.N., 2000. Contribution of remote sensing to drought early warning. In: Wilhite, D.A., Sivakumar, M.V.K., Wood, D.A. (Eds.), Improving Drought Early Warning Systems in the Context of Drought Preparedness and Mitigation. , pp. 65–85, Lisboa, Portugal, 86–100.

Kogan, F.N., 1995a. Droughts of the late 1980 in the United States as derived from NOAA polar-orbiting satellite data. Bulletin of the American Meteorological Society 76 (5), 655–668.

Kogan, F.N., 1997. Global drought watch from space. Bulletin of the American Meteorological Society 78 (4), 621–636.

Kogan, F.N., Stark, R., Gitelson, A., Jargalsaikhan, L., Dugrajav, C., Tsooj, S., 2004. Derivation of pasture biomass in Mongolia from AVHRR-based vegetation health indices. International Journal of Remote Sensing 25 (14), 2889–2896.

Kogan, F.N., 1995b. Application of vegetation index and brightness temperature for drought detection. Advances in Space Research 11, 91–100.

Kuhnert, M., Alexey, V., Ralf, S., 2005. Comparing Raster map comparison algorithms for spatial modeling and analysis. Photogrammetric Engineering and Remote Sensing 71 (8), 975–984.

Liu, W.T., Negron-Juarez, R.I., 2001. ENSO drought onset prediction in northeast Brazil using NDVI. International Journal of Remote Sensing 22, 3483–3501.

Mayaux, P., Bartholom, E., Cabral, A., Cherlet, M., Defourny, P., Di Gregorio, A., Diallo, O., Massart, M., Nonguierma, A., Pekel, J.-F., Pretorius, C., Vancutsem, C., Vasconcelos, M., 2003. The Land Cover Map for Africa in the Year 2000. GLC2000 Database. European Commission Joint Research Centre http://www-gem.jrc.it/glc2000

McKee, T.B., Doesken, N.J., Kleist, J., 1993. The relationship of drought frequency and duration to time scales. In: Preprints, 8th Conference on Applied Climatology, 17–22 January 1993, Anaheim, CA, pp. 179–184.

McKee, T.B., Doesken, N.J., Kleist, J., 1995. Drought monitoring with multiple time scales. In: Preprints, 9th Conference on Applied Climatology, January 15–20, Dallas, TX, pp. 233–236.

Mozafari, G.A., Khosravi, Y., Abbasi, E., Tavakoli, F., 2011. Assessment of geostatistical methods for spatial analysis of SPI and EDI Drought Indices. World Applied Sciences Journal 15 (4), 474–482.

Naciri, M., 1985. Calamites naturelles et fatalites historiques. In: Conf. Sécheresse, Gestion des Eaux et Production Alimentaire, Agadir (Morocco), pp. 83–101.

Naumann, G., Barbosa, P., Carrao, H., Singleton, A., Vogt, J., 2012. Monitoring drought conditions and their uncertainties in Africa using TRMM data. Journal of Applied Meteorology and Climatology 51, 1867–1874.

Palmer, W.C., 1965. Meteorological drought., pp. 58, U.S. Department of Commerce Weather Bureau Research Paper No. 45.

Peters, A.J., Walter-Shea, E.A., Lei, J., Vina, A., Hayes, M., Svoboda, M.R., 2002. Drought monitoring with NDVI-based standardized vegetation index. Photogrammetric Engineering and Remote Sensing 68 (1), 71–75.

Pontius Jr., R.G., Millones, M., 2011. Death to Kappa: birth of quantity disagreement and allocation disagreement for accuracy assessment. International Journal of Remote Sensing 32 (15), 4407–4429.

Pontius, R.G., 1994. Modeling Tropical Land Use Change and Assessing Policies to Reduce Carbon Dioxide Release from Africa, Graduate Program in Environmental Science. SUNY-ESF, Syracuse, NY, pp. 177.

Pontius Jr., R.G., 2000. Quantification error versus location error in comparison of categorical maps. Photogrammetric Engineering and Remote Sensing 66, 1011–1016.

Quiring, S.M., Ganesh, S., 2010. Evaluating the utility of the, Vegetation Condition Index (VCI) for monitoring meteorological drought in Texas. Agricultural and Forest Meteorology 150, 330–339.

Rhee, J., Im, J., Carbone, G.J., 2010. Monitoring agricultural drought for arid and humid regions using multi-sensor remote sensing data. Remote Sensing of Environment 114, 2875–2887.

Rojas, O., Vrieling, A., Rembold, F., 2011. Assessing drought probability for agricultural areas in Africa with coarse resolution remote sensing imagery. Remote Sensing of Environment 115 (2), 343–352, 15 February.

Rouse, J.W., Haas, R.H., Schell, J.A., Deering, D.W.,1973. Monitoring vegetation systems in the great plain with ERTS. In: Proceedings of the 3rd ERTS Symposium. US Governement Printing Office, NASA, Washington, DC, pp. 309–317.

Singh, R.P., Roy, S., Kogan, F.N., 2003. Vegetation and temperature condition indices from NOAA-AVHRRA data for drought monitoring over India. International Journal of Remote Sensing 24 (22), 4393–4402.

Son, N.T., Chen, C.F., Chen, C.R., Chang, L.Y., Minh, V.Q., 2012. Monitoring agricultural drought in the Lower Mekong Basin using MODIS NDVI and land surface temperature data. International Journal of Applied Earth Observation and Geoinformation 18, 417–427, August.

Udelhoven, T., Stellmes, M., del Barrio, G., Hill, J., 2009. Assessment of rainfall and NDVI anomalies in Spain (1989–1999) using distributed lag models. International Journal of Remote Sensing 30 (8), 1961–1976.

WMO, 2009. Copenhagen déclaration, Geneva, 15 December 2009. Press release No. 872 http://www.wmo.int/pages/mediacentre/press_releases/pr_872_en.html

Wood, J.M., 2007. Understanding and computing Cohen's Kappa: a tutorial. WebPsychEmpiricist http://wpe.info/

Wu, J., Zhou, L., Liu, M., Zhang, J., Leng, S., Diao, C., 2013. Establishing and assessing the Integrated Surface Drought Index (ISDI) for agricultural drought monitoring in mid-eastern China. International Journal of Applied Earth Observation and Geoinformation 23, 397–410, August.

Zhang, A., Jia, G., 2013. Monitoring meteorological drought in semiarid regions using multi-sensor microwave remote sensing data. Remote Sensing of Environment 134, 12–23, July.